Identification of a load model for crowd-rhythmic activities based on acceleration measurements of a building floor

Youssef El Asri[a,b,c], Mladen Lukić[a], Mohammed Hjiaj[b*], Maël Couchaux[b], Vincent Denoël[c]

a. Centre Technique Industriel de la Construction Métallique (CTICM), Espace Technologique l'Orme des Merisiers, Immeuble Apollo, 91193 Saint-Aubin, France
b. Institut National des Sciences Appliquées (INSA) de Rennes, 20 avenue des Buttes de Coësmes, 35708 Rennes Cedex 7, France
c. Université de Liège, Quartier Polytech 1, Allée de la découverte, 9, 4000 Liège, Belgium

***** Corresponding author. E-mail address: Mohammed.Hjiaj@insa-rennes.fr

Abstract

The floors of modern buildings are prone to excessive vibrations induced by human actions, especially when a group of people perform rhythmic activities in a coordinated manner. A reliable model for this load case, taking into account the experimentally observed group effect, is thus essential for the serviceability assessment of such structures. In this paper, a frequency-domain load model for either a single person or multiple individuals was established for two rhythmic activities. The model parameters were determined by an indirect identification method from acceleration responses. An extensive experimental test campaign was conducted on a steel–concrete composite floor in order to provide input data for identification, including experimental modal analysis and human-induced vibration tests for up to 32 individuals. The load parameters were first determined for the single-person load model. Root Mean Square (RMS) forces were then calculated from the identified load models, and corresponding coordination factors as a function of crowd size are suggested. A decreasing exponential was obtained for up to 8 persons for skipping and 12 persons for jumping, followed by a constant plateau for larger groups. The proposed models involve a global coordination factor to be used in conjunction with the identified model corresponding to skipping and jumping activities. A comparison of the proposed model and three existing coordination factor models against experimentally identified forces was performed. The comparison revealed the accuracy of the suggested models with respect to experimentally identified forces, whereas differences to existing factors were found especially for jumping.

Keywords: building floor, human-induced vibration, rhythmic load model, group effect, force identification, serviceability analysis.

1 Introduction

Progress in construction has led to significant changes in the performance of building floors. In fact, these structures are becoming more lightweight, slender and flexible due to the growing use of materials with high strength properties but low weight. Architectural considerations together with an increasing trend toward open spaces have also contributed to this situation. As a result, some serviceability issues have emerged in general cases, especially for floors subjected to human activities (walking, running, skipping, jumping, etc.) where occupants can feel discomfort from floor vibrations. The most relevant load case causing this effect is human-induced rhythmic loading, especially when a group of people excite the floor with a high level of synchronization. An et al. [1] highlighted this phenomenon by conducting an experimental investigation of an innovative composite floor subjected to human-induced vibrations. They confirmed that crowds jumping synchronously produced the greatest acceleration responses among the rhythmic activities studied. The impact of these actions could be even more pronounced: Lee et al. [2] demonstrated that crowd-rhythmic movements in a fitness centre located on the 12th floor of a 39-storey steel building in Seoul resulted in a 10-min vertical shaking episode causing panic to the occupants. Therefore, reliable load models for crowd-rhythmic activities are a prerequisite for the vibration serviceability assessment of floors.

Several attempts to develop such models have been made. Crowd models proposed in the literature were first based on a single person practicing rhythmic movements on the floor. Then, crowd effects observed in real situations (due to physical constraints, visual cues from crowd movement, stimulation from near environment [3], etc.) were investigated experimentally. A straightforward method for handling this is to conduct direct measurements of the force induced by each person on the floor. Dynamic load factors (DLFs) characterizing Fourier series models may then be determined for various rhythmic activities [3],[4]. Moreover, coordination factors [5] reflecting the lack of synchronization between individuals were proposed as a function of crowd size. The main rhythmic activity analysed was jumping, and several relations describing the variation in group loads against crowd size were derived, either for Fourier series models [6][7] or jumping pulse models [8]. Nevertheless, measuring single forces produced by each individual is not practical for the case of large crowd sizes. In fact, the maximum number of individual load plates used for such experiments was 15, as stated by Comer et al. [3]. The limited area of the force plate also restricts the movement of the individual, who may not be able to perform the activity in a comfortable manner. Alternatively, one can extrapolate results obtained with smaller crowd sizes or undertake simulations of larger crowds with a single-person model. However, these approaches do not capture the experimental crowd effects mentioned earlier.

Indirect determination of force parameters from measured responses on the floor was used instead, offering the possibility of analysing the group effect for larger crowds in real-life conditions without restricting their motion. Time-domain force reconstruction methods, widely used in structural dynamics for various loads [9][10], have been proposed for human-induced excitation. Dynamical systems were usually represented using a state–space description, and algorithms to identify unknown forces were based on various Kalman filter formulations [11],[12]. However, the estimation of input forces by these filter-type techniques is often contaminated by low-frequency drifts due to the integration of noisy response measurement in the identification process [13]. A sequential Bayesian approach based on a real-time noise updating was established to correct this issue [14]; however, this method is highly sensitive to the sampling interval, and potential inaccuracies could arise from approximations introduced for the temporal discretization [13].

Most of the load models representing rhythmic activities were expressed in the time domain, characterized by sharp peaks at each harmonic. This enables the excitation of only one dominant mode of vibration at once. However, building floors encountered in practice generally have multiple dominant modes, and some have closely spaced modes such as for multi-span or multi-panel floors [15],[16], indicating that time-domain models would not provide accurate results for these structures. Frequency-domain modelling is a good alternative to overcome this limitation [17], as it offers an excitation frequency window that can excite multiple close modes simultaneously. A proposal for the use of this model in the context of a random field approach was made by Xiong and Chen [18] for regular crowd jumping. It was based on the measurement of loads produced by 48 persons exciting a rigid floor using 3D motion capture technology. Although more reliable for characterizing group-induced loads, the implementation of this model is quite laborious and the generation of load parameters for every person in the group is time consuming. A simplified frequency-domain load model for rhythmic activities along with an adequate identification method from the measured responses on building floors are thus one of the key elements to be provided in this field of research.

In this paper, a frequency-domain load model characterizing two rhythmic activities is established for either a single person or multiple individuals exciting a floor structure. The parameters of this model are determined from experimental acceleration measurements using the least-squares identification technique. Experimental tests of a steel–concrete composite floor are presented along with the results. The background of the parametric identification method used for rhythmic loads is summarized, comprising the formulation of load models and response analysis procedures. Moreover, the load parameters are determined for the case of a single person, and the group effect is studied for multiple individuals. This is done by means of Root Mean Square (RMS) forces computed from the identified load models, providing relationships between RMS forces and crowd sizes. Finally, a comparison is made between the predictions of the proposed coordination factor models and those of three existing models for rhythmic activities against experimentally identified forces, and the findings are discussed.

2 Experimental set-up

An experimental program was performed in order to provide reliable data to be used in human-induced load identification for individuals and crowds. It comprised two test campaigns of a flexible floor: modal analysis and human-induced vibration tests [19].

2.1 Tested structure

Experimental tests were carried out on a three-storey composite steel and concrete parking structure located in Nantes, France (Fig. 1). The tested floor was located at 3 m above the ground and had a total area of approximately 4200 m². A rectangular area of 22.5 × 15.785 m² near the centre of the floor was selected for testing. It was made of a composite concrete deck of 130 mm thickness, with a 0.75-mm-thick profiled steel sheet of Cofraplus 60 type. The composite floor was supported underneath by welded I-members, and connection was achieved by shear studs of 19 mm diameter and 100 mm height. The secondary beams consisted of a 500×5 web and 150×12 flanges. The primary beams consisted of a 470×8 web and 200×15 flanges except for two beams with a 480×6 web and 150×10 flanges. The columns were composed of hot-rolled HEB340 profiles. All beams were assumed to be simply supported.

Fig.1: Composite steel and concrete parking floor in Nantes (France).

2.2 Modal analysis

The first test campaign aimed at characterizing the modal properties of the floor using Experimental Modal Analysis (EMA) [20]. The structure, having a considerable mass, was excited by a digitally controlled electrodynamic shaker (Fig. 2(a)), equipped with a 230 kg mass moving vertically with an amplitude of 0.5 or 1 mm. The shaker was consecutively placed at two positions, labelled “Setup 1” and “Setup 2” in Fig. 2(b). For each position of the shaker, white noise excitation enabled the detection of natural frequencies ranging between 3 and 10 Hz, which is within the range of frequencies of human excitation [21]. Then, the frequency of excitation was tuned to each natural frequency detected and the responses were measured by wireless accelerometers, having a sampling frequency of 64 Hz and a measurement range of ± 2 g. The accelerometers were placed on the floor structure at different locations (Fig. 2(b)). Synchronous measurement of the acceleration near the shaker (with an accelerometer having a measurement range of ± 2 g) provided Frequency Response Functions (FRFs) that are necessary for determining the modal properties (natural frequency, modal mass, damping ratio) of the floor by a curve fitting procedure. Relative accelerations (to the maximum value) made it possible to determine the modal shapes in the studied area.

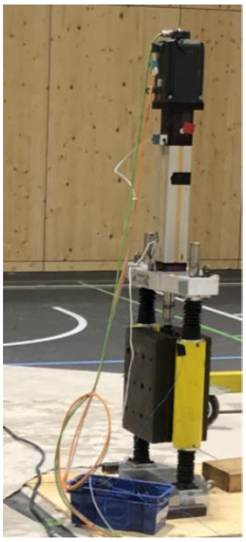

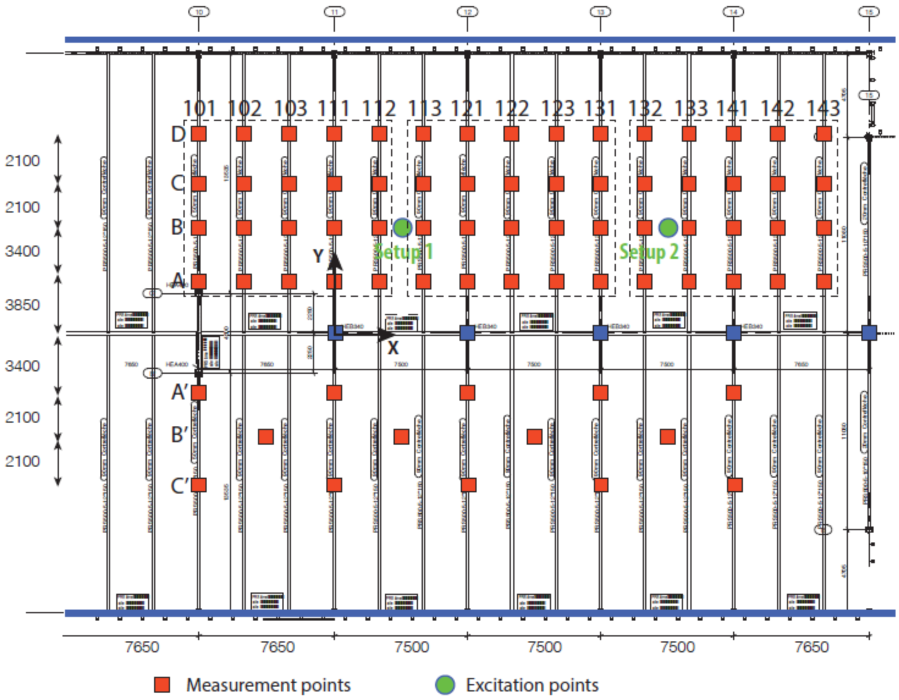

(a) (b)

Fig. 2: Experimental modal analysis set-up: (a) electrodynamic shaker; (b) positions of the shaker and accelerometers.

Data analysis revealed the existence of 20 closely spaced vibration modes with natural frequency ranging between 3 and 10 Hz. The structure is thus a relatively low-frequency floor [22], sensitive to human excitation. Examples of modal shapes identified for four different modes are shown in Fig. 3. Mode 1 is a global mode, whereas higher modes are more local.

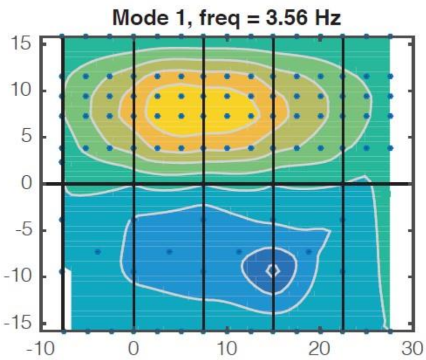

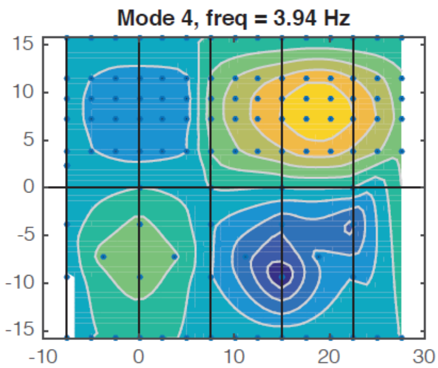

(a) (b)

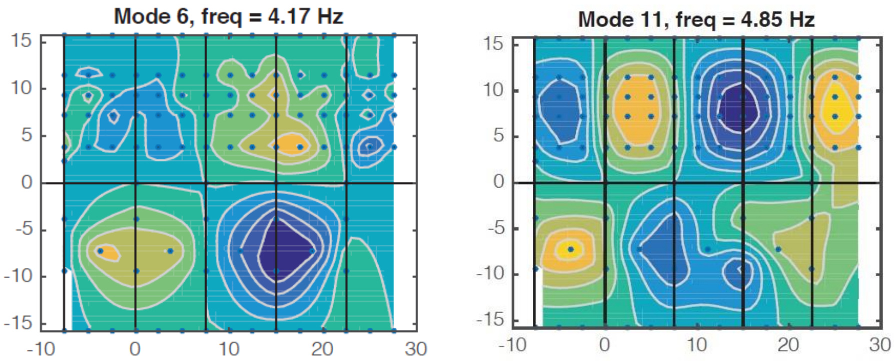

(c) (d)

Fig. 3: Identified modal shapes: (a) mode 1; (b) mode 4; (c) mode 6; (d) mode 11.

Solid black lines represent supporting beams. Dimensions are in metres.

Natural frequencies, modal masses and damping ratios of the modes illustrated in Fig. 3 are summarized in Table 1.

Table 1: Modal parameters of the floor.

Mode	Frequency (Hz)	Modal mass (t)	Damping ratio (%)
1	3.56	297	0.44
4	3.94	167	0.57
6	4.17	150	0.61
11	4.85	98	0.70

2.3 Human-induced vibration tests

A series of tests were conducted to measure the floor acceleration under two human-induced rhythmic loads: skipping (running at a fixed place) and jumping jacks, called “jumping” in this paper. Since it was considered that substantial effects in loads and responses would be observed through stepwise changes of group size [21], tests were conducted considering six series of one, two, four, eight, 16, and 32 individuals, respectively.

Participants were requested to stay at fixed positions uniformly distributed over the floor (as illustrated in Fig. 4 for the case of 32 persons). The crowd density was 0.16 person/m², which corresponds to a low-range density of occupants [23]. Individuals participated in rhythmic activities under the guidance of an experienced sports coach in order to represent a level of synchronization as close as possible to real situations. The tests were divided into two set-ups, each having specific crowd sizes, duration and a repetition number of activities, as presented in Table 2.

Table 2: Parameters of each set-up for vibration tests.

Set-up	Crowd size	Duration	Repetition
1	1, 16, 32	1 min	9 times
2	2, 4, 8	1 min	6 times

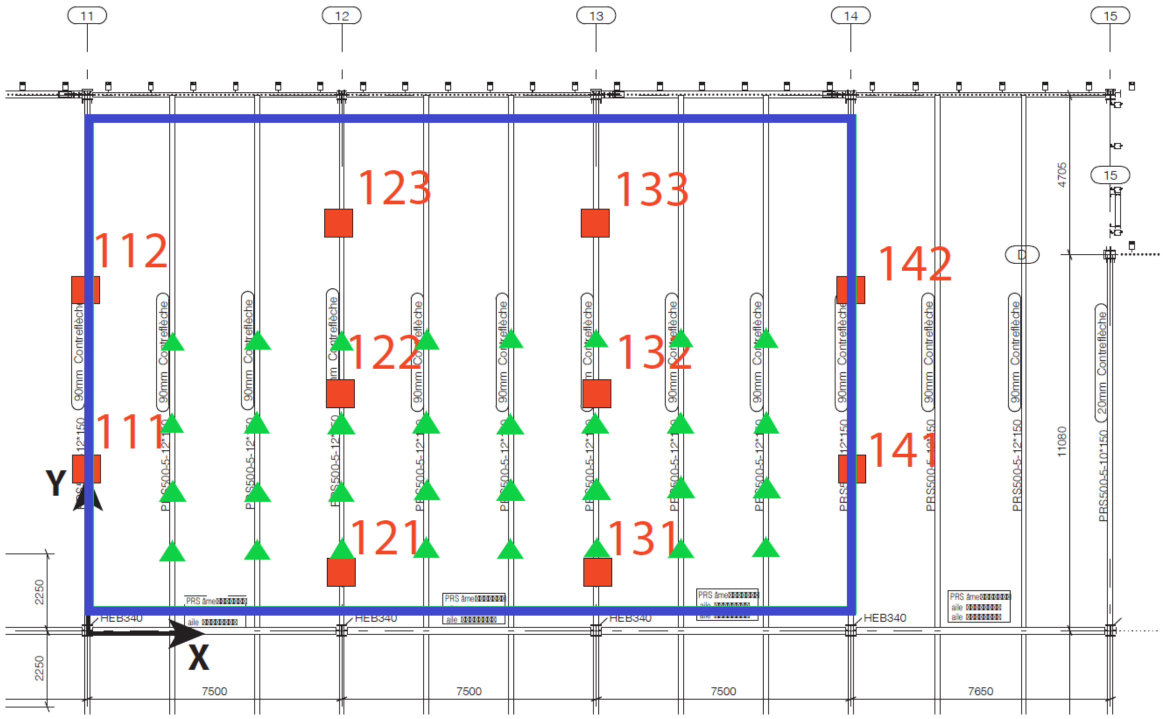

Fig. 4: Monitored area (blue box); positions of 32 individuals for rhythmic activities (green triangles); locations of accelerometers (red rectangles).

A total of 35 participants (26 men and nine women) were involved in this campaign. The test procedure was briefly described to all participants prior to starting the activities. Their ages ranged from 18 to 58 years (mean: 28 years, standard deviation: 12 years) and their weights (measured at the beginning of the test) varied from 52.3 to 126.6 kg (mean: 75.8 kg, standard deviation: 15.4 kg). Fig. 5 shows the 32 individuals skipping on the floor.

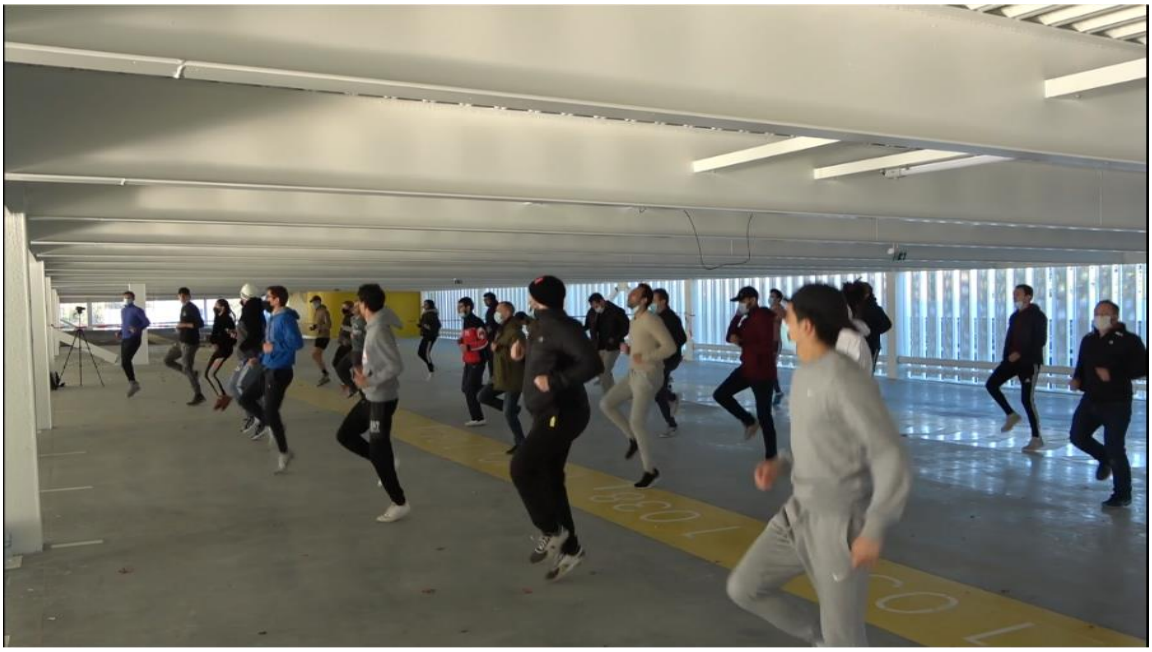

Fig. 5: 32 individuals skipping on the tested floor.

2.4 Response measurements

Floor accelerations induced by human activities were measured using 10 cabled accelerometers with a sampling frequency of 256 Hz. They were installed on the secondary beams of the tested floor at different locations (Fig. 4). A total of 2.5 h of response data was recorded during this campaign. An illustration of the accelerations measured by accelerometer no.°111 (Fig. 4) is presented in Fig. 6 for four individuals performing skipping and jumping activities.

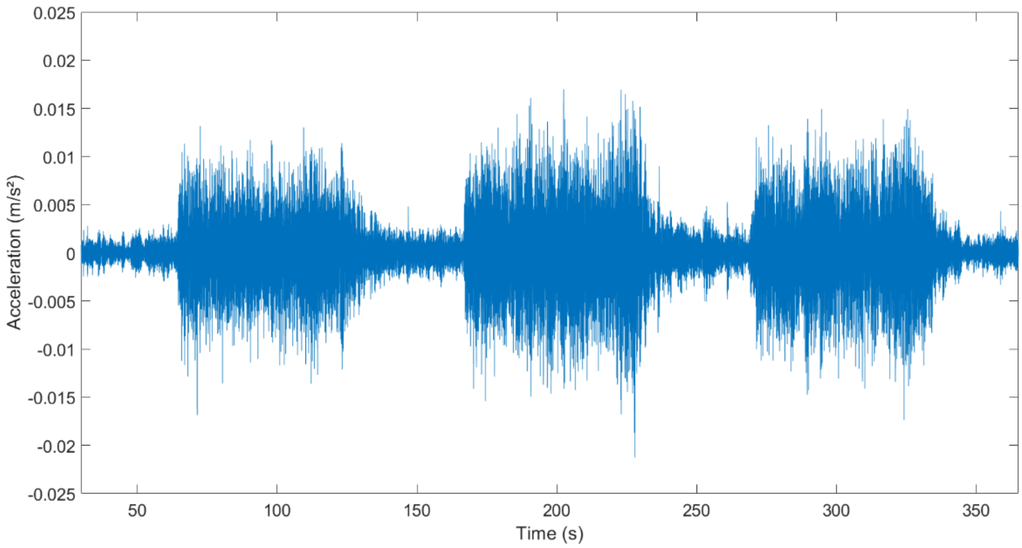

(a)

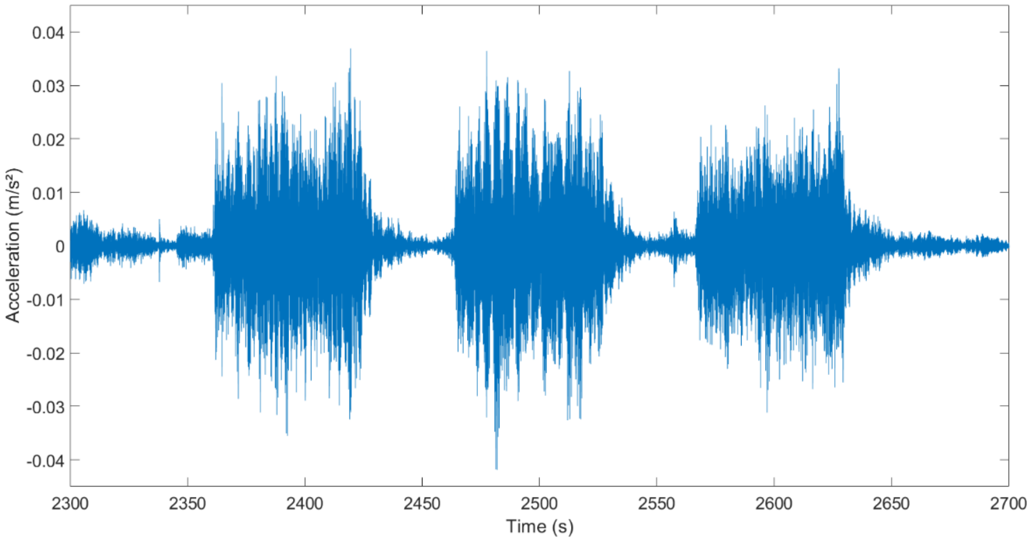

(b)

Fig. 6: Accelerations measured by accelerometer no.°111 for four individuals: (a) skipping; (b) jumping.

Acceleration recordings due to rhythmic activities were processed using MATLAB. For each activity, structural responses were extracted on the basis of an automatic envelope detection, which is simply implemented using a Hilbert transform. The envelope corresponding to each time window was truncated by 5 s at the beginning and at the end of each signal to keep the stationary response only and to match with the slot where all individuals were moving according to the protocol. Each recording was then filtered within the frequency range between 0 and 10 Hz via Fast Fourier Transform (FFT). An example of a filtered acceleration signal for skipping activity extracted from the recording shown in Fig. 6 is illustrated in Fig. 7 in the time and frequency domains.

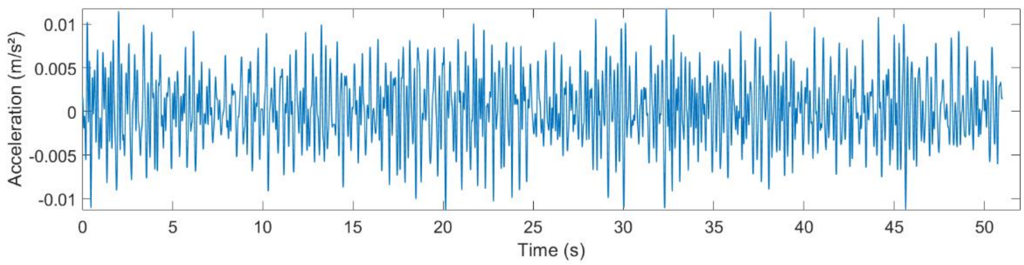

(a)

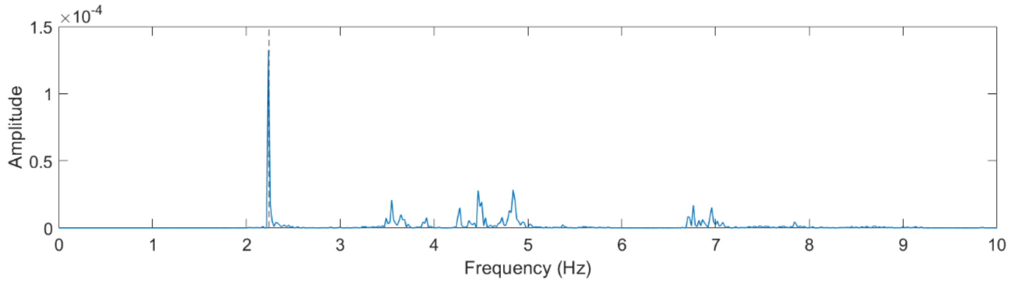

(b)

Fig. 7: Acceleration signal for four individuals skipping: (a) time domain; (b) frequency domain.

3 Background for rhythmic load identification

After having identified modal parameters of the floor structure, the latter was subjected to rhythmic activities by individuals (with known masses) located at known fixed positions. Corresponding accelerations were measured at pre-defined response points. In order to determine the loads that produced the floor accelerations, a parametric load model was established either for a single person or multiple individuals. It is noted that only the dynamic part of human loads was considered since quasi-static response is not measured by accelerometers. The method for evaluating the response of floors subjected to rhythmic activities is presented afterwards.

3.1 Rhythmic load model

In this study, a frequency-domain model for rhythmic activities is adopted considering a specific Power Spectral Density (PSD) formulation. The proposed load model takes into account the variation of excitation frequency during movement (“intra-subject variability”).

3.1.1 Single-person load model

The PSD load model from an existing random field approach for jumping [18] is expressed for each harmonic i by:

$$S_{p,i}(f) = (mg)^2 \left(\frac{\rho S_i}{i f_p}\right) \left[p_5 \exp\left(-\left[\left(\frac{f - i f_p}{i f_p p_6}\right)\right]^2\right) + p_7 \exp\left(-\left[\left(\frac{f - i f_p}{i f_p p_8}\right)\right]^2\right)\right] \quad (1)$$

where the corresponding parameters are described in [18].

Fig. 8 illustrates the PSD model using three harmonics, for an individual weighing 75 kg and jumping at 2 Hz.

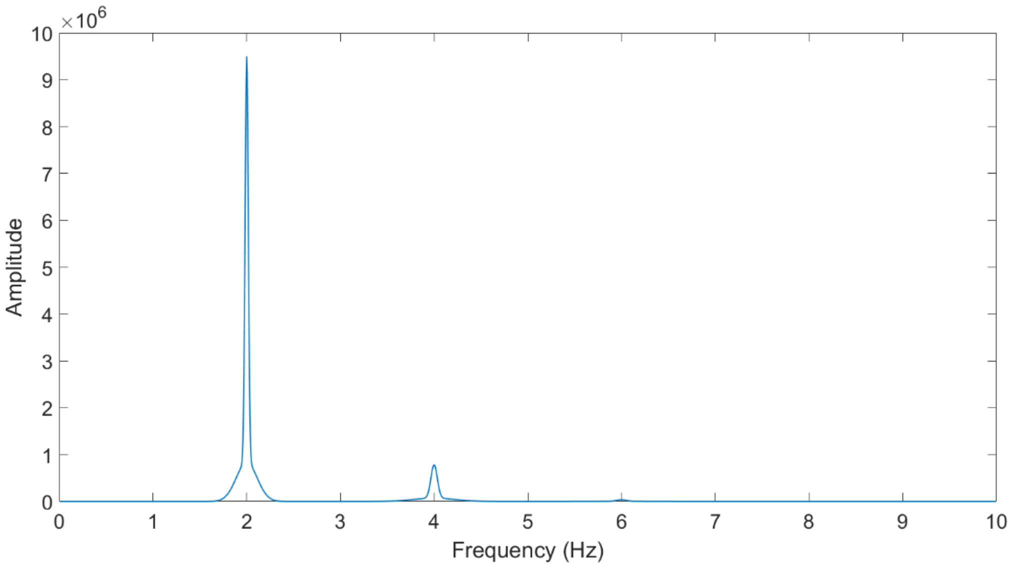

Fig. 8: PSD load model obtained from [18] (75-kg individual and 2 Hz excitation frequency)

We note that the exponential function (given in Eq. (1)) accurately models the frequency content at each harmonic. In fact, it has a bell shape enabling a gradual decrease in amplitude, which represents the spread of energy (leakage) in the vicinity of the peak of each harmonic [24]. As a consequence, the proposed formulation assumes that each harmonic can be modelled by a unique exponential function given by:

$$S_{p,i}(f) = (mg\alpha_i)^2 \exp\left(-\frac{(f - if_p)^2}{\delta_i^2}\right) \tag{2}$$

where m is the mass of the participant, g the gravity acceleration (equal to 9.81 m/s²), f_p the excitation frequency, α_i an amplitude coefficient of the i^{th} harmonic and δ_i a coefficient defining the leakage of energy from the frequency centres of each harmonic if_p [24]. The total PSD load model is then deduced for H harmonics by:

$$S_p(f) = \sum_{i=1}^{H} S_{p,i}(f) \tag{3}$$

The PSD load model given by Eq. (2) was simplified for skipping and jumping activities in order to have a limited number of parameters for identification. In fact, three harmonics (H = 3) were considered for each activity, since it covers the maximum frequency range of human activities (between 0 and 10 Hz) [21]. The coefficient δ_i was taken from the aforementioned random field model for jumping activity [18] where it is evaluated according to the following expression: $\delta_i = i\delta_1$. The ratio between amplitude coefficients $a_i = \alpha_i/\alpha_1$ was assumed to be the same as that for the dynamic load factors (DLFs) of an equivalent time-domain load model.

Pernica [4] conducted an experimental study to extract time-domain load parameters (especially DLFs) for several human activities, including running-on-the-spot and stride jumps, which correspond to skipping and jumping as performed in our experiments, respectively.

Each load model is decomposed in a Fourier series as follows:

$$P(t) = mg\left[\sum_{i=1}^{3} DLF_i \sin\left(2\pi i f_p t\right)\right] \tag{4}$$

These loads are one of the most widely used models from the literature reproducing experimental activities. DLFs for these two load models are provided in Table 3.

Noting $\delta_1 = \delta$ and $\alpha_1 = \alpha$, the PSD load model can be simplified by the following expression:

$$S_p(f) = (mg\alpha)^2 \sum_{i=1}^{3} \left[a_i^2 \exp\left(-\frac{(f - if_p)^2}{(i\delta)^2}\right)\right] \tag{5}$$

where the relative parameters a_i (i=1, 2, 3) are given in Table 3. Parameters to be identified for each activity are then f_p, α and δ.

Table 3: Load parameters DLF_i [4] and a_i for skipping and jumping.

Activity	DLF_1	DLF_2	DLF_3	a_1	a_2	a_3
Skipping	1.57	0.58	0.26	1	0.4	0.15
Jumping	1.75	1.1	0.42	1	0.6	0.25

3.1.2 Crowd load model

The load model characterizing crowd-rhythmic activities is modelled using a random field approach [18]. For N individuals rhythmically exciting the floor structure, each person on an excitation point k is assumed to have a PSD load model noted $S_{p,k}(f)$. In reality, these persons perform rhythmic activities in a different manner depending on the style of each individual's movement ("inter-subject variability"). The interaction of each pair of individuals is then expressed by a coherence function. For the proposed PSD load model, this is taken into account by assuming a complete coherence function, which is corrected by coordination factors reflecting the reduction of crowd loads due to the lack of synchronization between individuals [5]. The correction is determined after the identification of load parameters f_p, α and δ for each activity window (assumed to be identical for all participants).

Hence, the PSD force matrix for a group of N individuals $[S_{p,N}(f)]$ ($N \times N$) is defined by [18]:

$$\left[S_{p,N}(f)\right]_{k,l} = \begin{cases} S_{p,k}(f), & k = l \\ S_{p,k,l}, & k \neq l \end{cases} \tag{6}$$

where $S_{p,k}(f)$ is the PSD load model for a person in the group and $S_{p,k,l}(f)$ the cross-PSD model between the k^{th} and l^{th} persons.

For an individual having a known mass m_k, the PSD model $S_{p,k}(f)$ is expressed by:

$$S_{p,k}(f) = C(N)^2\, S_p(f) \tag{7}$$

Here, $S_p(f)$ is the PSD load model for a single person exciting the floor obtained by Eq. (5) and $C(N)$ the coordination factor related to crowd size N.

On the other hand, the cross-PSD load model $S_{p,k,l}(f)$ is given by:

$$S_{p,k,l}(f) = \sqrt{S_{p,k}(f) S_{p,l}(f)} \tag{8}$$

3.2 Response of floors to rhythmic activities

Major steps for the calculation of the floor response due to rhythmic activities are provided next. Further details can be found in [25].

For a number n_m of natural modes of the floor, the PSD matrix of generalized forces $\left[S_{p*}(f)\right]$ ($n_m \times n_m$) is given by:

$$\left[S_{p*}(f)\right] = [\Phi_p^T]\,\left[S_{p,N}(f)\right]\,[\Phi_p] \tag{9}$$

where $[\Phi_p]$ is the matrix of modal amplitudes at the excitation points ($N \times n_m$).

The uncoupled equations of motion for each natural mode n are:

$$\ddot{q}_n(t) + 2\xi_n\omega_n\dot{q}_n(t) + \omega_n^2 q_n(t) = \frac{1}{M_n} p_n{}^*(t) \tag{10}$$

where ω_n, M_n, ξ_n, q_n and $p_n{}^*$ are the circular frequency, modal mass, damping ratio, modal coordinate and generalized force for the n^{th} mode, respectively. Combining Eq. (10) for all modes in the frequency domain gives the PSD matrix of modal coordinates related to displacement $\left[S_q(f)\right]$ ($n_m \times n_m$) as follows:

$$[S_q(f)] = [H(\omega)][S_{p*}(f)]\overline{[H(\omega)]}^T \tag{11}$$

where $[H(\omega)]$ is the frequency response function (FRF) matrix ($n_m \times n_m$) defined for each circular frequency ω by:

$$[H(\omega)]_{n,n} = \frac{1}{M_n(\omega_n^2 - \omega^2 + 2i\xi_n\omega_n\omega)} \tag{12}$$

The PSD matrix of modal coordinates related to acceleration $[S_{\ddot{q}}(f)]$ is given by:

$$[S_{\ddot{q}}(f)] = \omega^4[S_q(f)] \tag{13}$$

Finally, for n_r response points, the PSD matrix of acceleration responses $[S_{\ddot{x}}(f)]$ ($n_r \times n_r$) is deduced by:

$$[S_{\ddot{x}}(f)] = [\Phi_r][S_{\ddot{q}}(f)][\Phi_r^T] \tag{14}$$

where $[\Phi_r]$ is the matrix of modal amplitudes at the response points ($n_r \times n_m$). Diagonal terms of $[S_{\ddot{x}}(f)]$ are arranged into a single column vector $\{S_a(f)\}$ of length n_r. The final response matrix $[S_a]$ ($n_r \times N_e$) is obtained by the combination of successive $\{S_a(f)\}$ columns, each calculated by the same method described earlier for N_e frequencies.

RMS accelerations were used as a response descriptor since it is a robust estimator of the human response to human-induced vibrations, justifying its adoption in many guidelines on evaluating human comfort [22] or defining acceptability limits for comfort [5]. Forces were also characterized by RMS values to have similar parameters for forces and responses. For a given parameter w (force or response) having a PSD vector noted $S_w(f)$, the corresponding RMS value is calculated by the following expression:

$$w_{rms} = \sqrt{\int_0^{+\infty} S_w(f)df} \tag{15}$$

4 Identification of single-person rhythmic load models

In order to define a crowd load model characterizing rhythmic activities, the PSD load model described in Section 3.1 for the case of a single person should be first determined. In this section, load parameters of the aforementioned model were experimentally identified for skipping and jumping activities. Acceleration records for the case of a single person (Section 2.4) were used for that purpose.

4.1 Least-squares fitting

Research works dealing with parametric identification from measured floor responses use the same method to identify, for each harmonic, the load parameters from the displacement [21] or the acceleration responses [26]. However, several simplifying assumptions related to the structure were made for that purpose (one principal mode of vibration, idealized modal shape, harmonic response, etc.). These methods were also based on time-domain load models that could not reproduce "intra-subject variability" effects observed during the experiments.

To circumvent these limitations, the proposed method aims to determine the load parameters of the frequency-domain model presented in Section 3.1. Optimization was based on a least-squares fitting applied to all types of floor structures (having multiple modes and various modal shapes). This was done by minimizing an objective function consisting in the squared norm of the difference between observations and model predictions in terms of acceleration responses. Parameters were identified using *lsqnonlin* solver that is available in the MATLAB Optimization toolbox. This solver is adapted to least squares problems based on nonlinear formulations, requiring two major inputs: an initial estimation of parameters and a function to be minimized. Solver calculates optimal parameters using the Levenberg–Marquardt algorithm along with Jacobian scaling to ensure stability. Details on the implementation of this technique for load model identification are provided in the next section.

4.2 Identification method

For N individuals rhythmically exciting the floor structure, the PSD load model described in Section 3.1 was adopted, characterized by load parameters f_p, α and δ. Identification was made for each type of activity and activity window j (of about 1-min duration) for the case of a single person. Parameters f_p and δ describing the shape of the PSD model were identified using PSD responses. Parameter α controlling the load amplitude was later identified using RMS acceleration responses. This two-step process was performed as follows:

4.2.1 Step 1: Identification of f_p and δ

The floor responses due to each activity window j, measured by accelerometers, were rearranged into the PSD matrix of measured responses and noted $[S_{a\_obs}]$. Noting $\theta = [f_p, \delta]$, response computation was performed using the proposed PSD load model (Eq. (5)) and the response analysis procedure of Section 3.2 (with dominant natural modes). This resulted in the PSD matrix of predictive responses noted $\left[S_{a\_pred}(\theta)\right]$. An initial value $\theta_{0,j}$ was chosen for the investigated parameters, and optimization was carried out (Section 4.1) in order to have:

$$\theta_{opt,j} = \underset{\theta}{\operatorname{argmin}} \left\| \left[S_{a\_pred}(\theta)\right] - [S_{a\_obs}] \right\|^2 \tag{16}$$

Resulting optimal vector $\theta_{opt,j}$ is considered valid if f_p ranges between 1.5 and 3.5 Hz [5],[22] and δ is within the interval [0.01, 0.2 Hz].

4.2.2 Step 2: Identification of α

The PSD load model became α-dependent with fixed f_p and δ values taken from the previous step, in order to ensure more precise identification in terms of RMS responses. We noted $\{a_{rms\_obs}\}$ as the experimental RMS acceleration vector and $\{a_{rms\_pred}(\alpha)\}$ as the predictive RMS acceleration vector, calculated from the α-dependent PSD matrix of forces using the response analysis method described in Section 3.2 (with dominant natural modes). These vectors were computed for all response points investigated, and optimization was performed (Section 4.1) to obtain:

$$\alpha_{opt,j} = \underset{\alpha}{\operatorname{argmin}} \left\| \{a_{rms\_pred}(\alpha)\} - \{a_{rms\_obs}\} \right\|^2 \tag{17}$$

4.2.3 Results

The method described in the previous sections was used to identify the PSD load model for both activities performed by a single person. The mean measured and predictive PSD responses (using the identified PSD model) for all accelerometers is illustrated for skipping and jumping activities in Fig. 9.

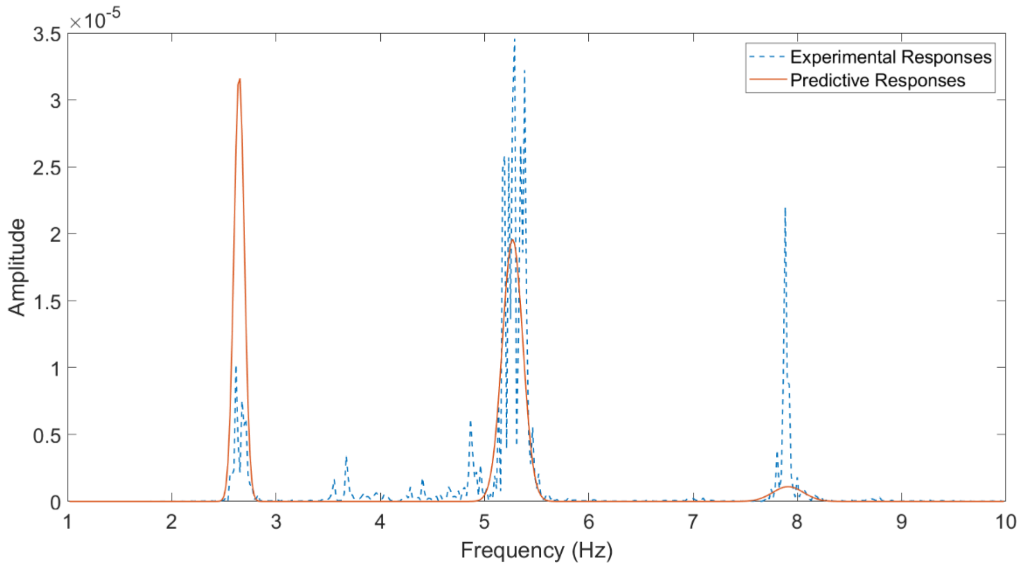

(a)

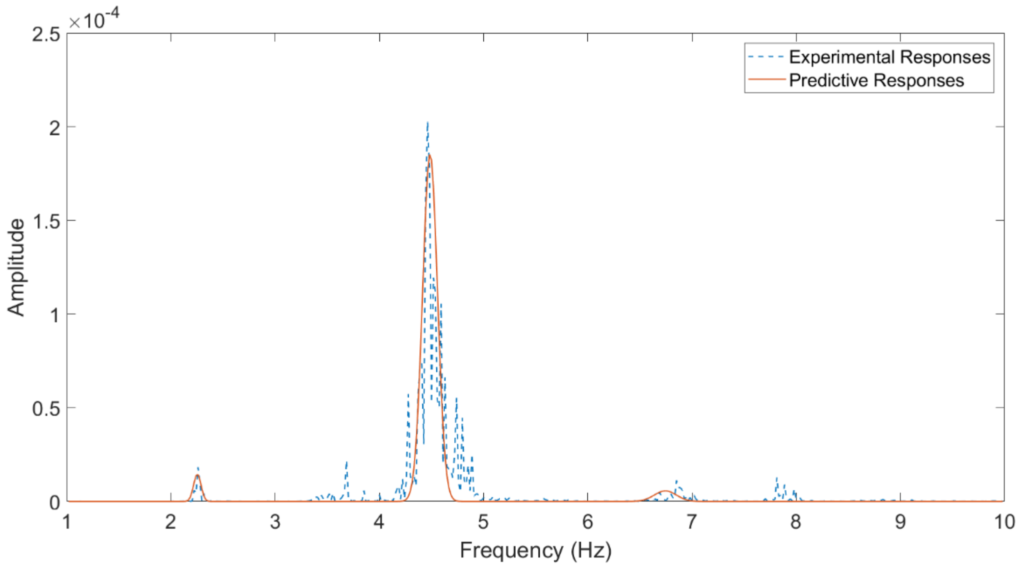

(b)

Fig. 9: Comparison of mean measured and predictive PSD responses for a single person: (a) skipping; (b) jumping.

The mean values and standard deviations of the identified load parameters f_p, α and δ obtained from all activity windows are provided in Table 4.

Table 4: Identified load parameters for a single person skipping and jumping.

Activity	f_p (Hz)	α	δ (Hz)
Skipping	2.62 ± 0.06	4.06 ± 1.40	0.062 ± 0.04
Jumping	2.19 ± 0.04	4.63 ± 2.07	0.037 ± 0.02

The PSD load models were evaluated using the mean parameters for both analysed activities, considering an individual having a body mass of 75 kg. The resulting RMS forces were 1166 N for skipping and 1205 N for jumping, indicating that more energy is produced when performing the second activity than the first.

It can be seen that the parameters of the PSD load models differ slightly between the studied activities. However, the identified excitation frequency indicates that jumping is a low-frequency activity whereas skipping is a high-frequency one. The standard deviation of parameters reveals that the parameter with the greatest fluctuation between activity windows is α, followed by f_p and then δ. This is due to the variable amount of impact made by the individual at each rhythmic sequence. The variability of parameters is generally more pronounced for skipping, because it exhibits more randomness in motion (similar to running) than jumping.

5 Crowd size effect on human-induced rhythmic loads

The influence of crowd size on human-induced rhythmic loads is analysed in this section, by identifying equivalent RMS forces based on the proposed PSD load model. Measurements of acceleration responses of all crowd sizes (from 1 to 32) for skipping and jumping activities were used for this purpose.

5.1 Method

Identification was performed for each type of activity, crowd size N and activity window j (of about 1-min duration). Each individual k had a known body mass m_k and a PSD load model $S_{p,k}(f)$ given by Eq. (7). Identical load parameters were adopted for all persons (Section 3.1.2).

The method detailed in Section 4.2 was used to identify optimal load parameters f_p, α and δ (Eq. (5)). RMS forces by activity window j and individual k (noted $F_{rms,j,k}$) were then calculated from the identified PSD load model $S_{p,k}(f)$ using Eq. (15). The combination of these values provided the equivalent RMS force of a single person being present in the group of N individuals, expressed as follows:

$$F_{rms,eq,j}(N) = \sqrt{\frac{1}{N}\sum_{k=1}^{N} F_{rms,j,k}^2} \tag{18}$$

The RMS forces obtained for all activity windows were then characterized by their mean values (noted $F_{rms,eq}(N)$) and standard deviations for each crowd size N.

The equivalent RMS force decreases with crowd size [5] due to considerations of group effect (restricted movement, lack of synchronization, etc.). As stated in Section 3.1.2, the relation between human-induced forces and crowd sizes is usually expressed in terms of coordination factors given by [5]:

$$C(N) = \frac{F_{rms,eq}(N)}{F_{rms,1p}} \tag{19}$$

where $F_{rms,eq}(N)$ is the equivalent RMS force for an individual within a group of N individuals and $F_{rms,1p}$ the individual's RMS force.

As a consequence, the evolution of equivalent RMS forces $F_{rms,eq}(N)$ with respect to crowd size N should be fitted by an appropriate decreasing relation. For the activities investigated here, it was found that the identified relative RMS forces exhibit a power tendency for smaller crowds.

Moreover, coordination between individuals was stabilized at almost the same level for larger crowds. Consequently, the relationship between coordination factors (given by Eq. (19)) and crowd size was best described by a function divided into two parts as follows:

$$C(N) = \begin{cases} N^{-r}, & 1 \leq N \leq N_0 \\ C_0, & N_0 < N \leq N_{max} \end{cases} \tag{20}$$

where $F_{rms,1p}$ is the individual's RMS force, r the group effect exponent, N_0 the crowd size limit between the two parts, C_0 the coordination factor for N_0 individuals and N_{max} the maximum investigated crowd size (32 for this study).

A least-squares curve fitting procedure using the *lsqcurvefit* function in MATLAB was performed to determine optimal parameters $F_{rms,1p}$ and r for a given value of N_0. The optimal value of N_0 with respect to RMS forces, providing an exponent r lower than 1 [21] and a determination coefficient R^2 greater than 0.9, was then determined.

5.2 Results

The resulting model parameters of Eq. (20) are summarized in Table 5.

Table 5: Model parameters for skipping and jumping.

Activity	r	N_0	C_0	R^2
Skipping	0.64	8	0.26	0.93
Jumping	0.53	12	0.27	0.98

Note: R^2 is the determination coefficient of regression laws

In Fig. 10, the identified equivalent RMS forces are plotted in conjunction with crowd size relations against the number of individuals.

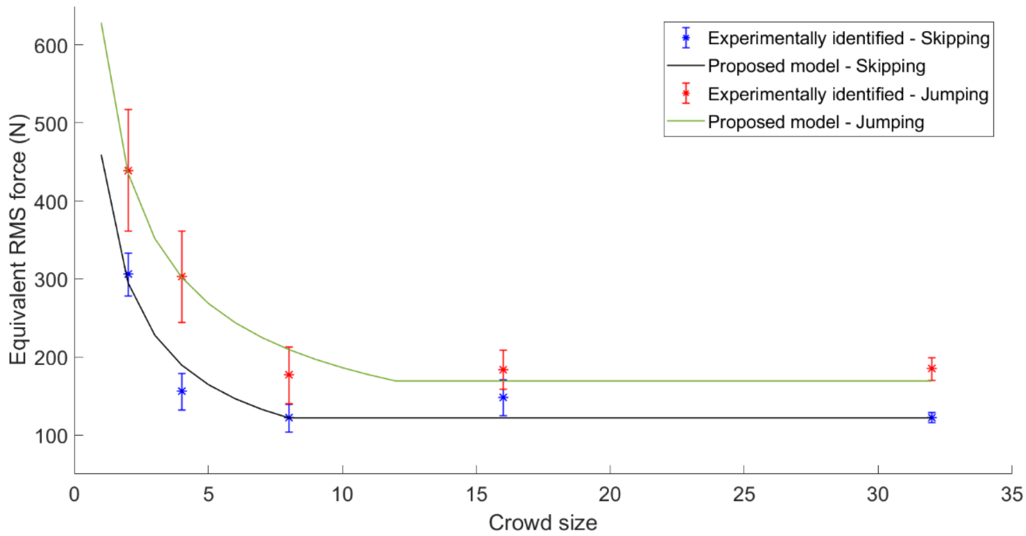

Fig. 10: Equivalent RMS forces against crowd size N including mean values and standard deviations (in error bars) along with regression curves (solid lines) for skipping and jumping.

The resulting curves provide a high-precision level for jumping (R^2=0.98) and skipping (R^2=0.93) for all crowd sizes. An exception to this is the case of four persons skipping, which presents lower identified values compared to their fitted counterparts. Since the fitting was made by an optimization procedure based on a least-squares technique, this case is considered to be an outlier and crowd size relations are then validated.

5.3 Discussion

For the first part of the proposed coordination factors, the group effect exponent for jumping is lower than that for skipping, indicating a smaller decrease of RMS forces with respect to crowd size N. This is because individuals reached a higher degree of synchronization in the first activity than in the second one. The power relation of rhythmic forces as a function of crowd size was also found by Ellis and Ji [21] but in terms of dynamic load factors (DLFs) for the first three harmonics. However, coordination factors continued decreasing for larger crowd sizes (up to 64). The existence of a constant group effect for larger crowd sizes was noted by Parkhouse and Ewins [7], who obtained squared DLF relations with a term proportional to $1/N$, providing constant coefficients for a huge number of persons, although coordination factors for crowds ranging between one and 32 persons were still decreased. For both models, each harmonic has specific model parameters showing a decrease in coordination factors by harmonic order, whereas the proposed model takes into account a more global group effect coefficient to be applied to the entire individual load.

As a result, the PSD force matrix for crowds expressed by Eq. (6) could then be deduced from the crowd model characterizing rhythmic activities given by Eq. (7) using:

- The PSD function expressed by Eq. (5), with optimal parameters taken from Table 4 (for the case of a single person);
- Coordination factors obtained by Eq. (20) for the case of crowds, with parameters given in Table 5.

6 Comparison with existing crowd models

6.1 Investigated crowd size models

Several crowd size models corresponding to rhythmic activities are available in the literature. For comparison purposes, three models either presenting a global coefficient or considering a constant group effect for larger crowd sizes were selected.

In the first model, proposed by Faisca (as stated by Costa-Neves et al. [16]), the equivalent force of a single person in a group of N participants $F_N(t)$ is expressed as follows:

$$F_N(t) = CD(N)F(t) \tag{21}$$

where $F(t)$ is the force produced by a single person and $CD(N)$ a phase coefficient depending on the activity considered and the group size N. This coefficient was obtained for two types of activity (aerobics, free jumps) and corresponding values for crowd sizes up to 32 are given in Table 6. The model associated with "Free jumps" was used for the jumping activity in the next comparison.

Table 6: Phase coefficient $CD(N)$ of Faisca's model by type of activity [16].

N	Aerobics	Free jumps
1	1	1
3	1	0.88
6	0.97	0.74
9	0.96	0.7
12	0.95	0.67
16	0.94	0.64
24	0.93	0.62
32	0.92	0.6

A second model was taken from the ISO 10137 standard [5] applied to coordinated rhythmic activities. The equivalent force related to a single person in a group of N individuals $F_{N,i}(t)$ is given for each harmonic i by:

$$F_{N,i}(t) = C_i(N)F_i(t) \tag{22}$$

where $F_i(t)$ is the i^{th} harmonic of the force of a single person and $C_i(N)$ a coordination factor depending on the i^{th} harmonic, the crowd size N and the considered activity.

For jumping, the coordination factor is given as follows:

- If $1 \leq N \leq 5$, , $C_i(N) = 1$;
- If $N \geq 50$, $C_i(N)$ depends on each harmonic and coordination degree (high, medium, low), as indicated in Table 7.

Table 7: Coordination factor of ISO 10137 for jumping [5].

Coordination	1st harmonic	2nd harmonic	3rd harmonic
High	0.8	0.67	0.5
Medium	0.67	0.5	0.4
Low	0.5	0.4	0.3

- If $5 < N < 50$, a linear interpolation between the two previous cases is applied.

The degree of coordination adopted in this model was considered as medium for jumping, similar to what was encountered in experiments. For skipping, the coordination factor related to running activity (similar in motion) was used for comparison, expressed by the following relation (for all harmonics):

$$C(N) = \frac{\sqrt{N}}{N} \tag{23}$$

A third model was established by Ebrahimpour and Sack [6] for jumping activity in terms of dynamic load factors (DLFs), where each DLF_i (of the i^{th} harmonic) is expressed as a function of the crowd size N by:

$$\begin{cases} qDLF_i = A_i - B_i N, & 1 \le N \le 10 \\ qDLF_i = C_i, & N > 10 \end{cases} \tag{24}$$

where q is the intensity of the individual's load (ratio of the individual's weight to the occupied surface) and parameters A_i, B_i and C_i are given for each harmonic i in Table 8.

Table 8: Parameters A_i, B_i and C_i (in psf) [6]

Harmonic	A_i	B_i	C_i
1st harmonic	50.89	1.89	32
2nd harmonic	20.89	0.89	12
3rd harmonic	4	0	4

6.2 Comparison of coordination factors

The coordination factor models proposed in this research (provided by Eq. (20) with results from Table 5) are evaluated against the aforementioned models from the literature. Predictions of these models are also compared against the experimentally identified RMS forces presented in Section 5.2. For the model proposed by Ebrahimpour and Sack [6], coordination factors are determined as the relative values of the equivalent crowd load to the individual's load for each harmonic. The resulting factors are plotted against crowd size N (for up to 32 individuals) in Fig. 11 for jumping and skipping activities. It can be observed that coordination factors have lower values for higher harmonics of the load.

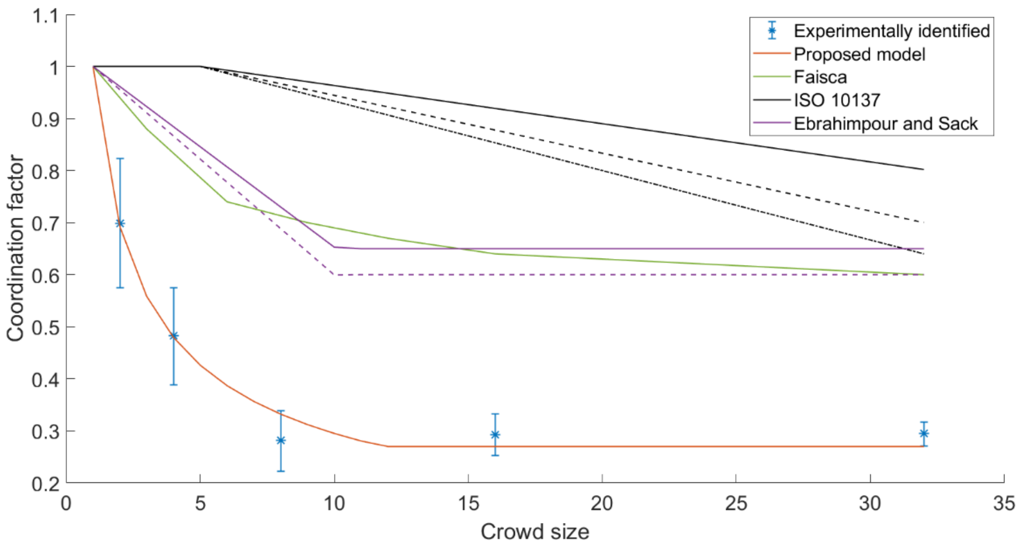

(a)

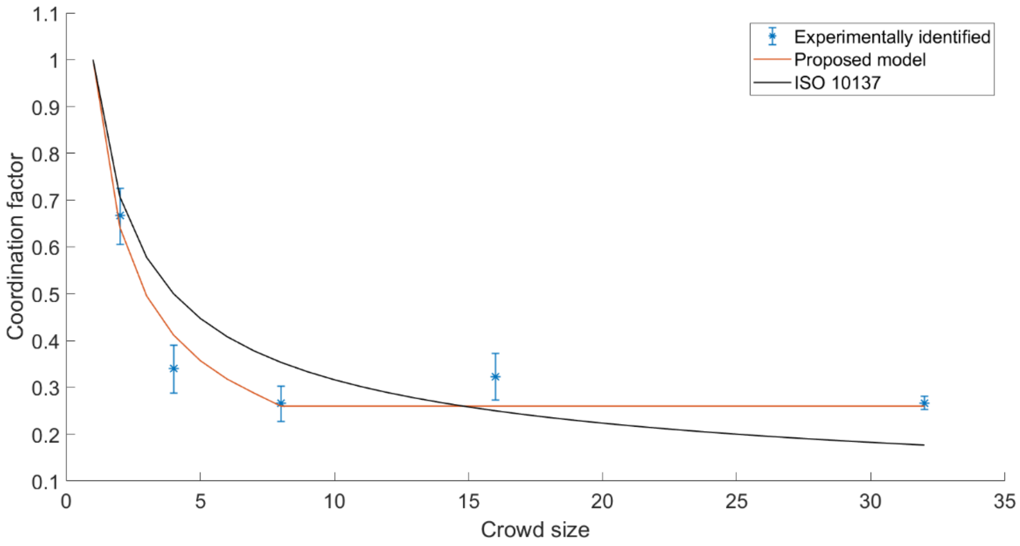

(b)

Fig. 11: Comparison of coordination factors against experimentally identified forces: (a) jumping; (b) skipping.

For jumping, higher harmonic relations are represented by dashed lines.

For jumping activity, the ISO 10137 model provides the highest crowd-size-dependent coordination factors. In this model, group effect on the synchronization of individuals is neglected for crowd sizes of less than five and the coordination factor is stabilized beyond 50 individuals, which is much larger than the 12 persons suggested as the crowd size limit in our study. The models proposed by Ebrahimpour and Sack, on one hand, and Faisca, on the other, result in lower factors, but still more severe than the values derived from the research described in this paper.

For skipping activity, the proposed model has lower coordination factors than the ISO 10137 model for smaller crowd sizes. However, the existence of constant plateau after eight individuals results in higher coordination factors suggested in this study compared to the ISO factors starting from 16 persons. This indicates that crowd forces may be underestimated for larger crowds if the ISO 10137 model is adopted.

In terms of floor response, Gaspar and da Silva [27] computed accelerations due to several load models applied on a composite floor. They highlighted that the load model proposed by ISO 10137 provided the maximum responses resulting in an unacceptable vibration level in terms of human comfort. On the other hand, the Faisca model presented acceptable floor accelerations, and corresponding load parameters could be adjusted to meet the specific characteristics of the jumping activity analysed. Following the same trend as for coordination factors, use of the Ebrahimpour and Sack model would result in floor accelerations lying between those obtained by the two previous models.

Overall, the proposed model, fitting well our experimental results, generally provides lower values than those given by the three existing models selected from the literature, especially for jumping. In fact, the exponential relation in the first part of the suggested model provides a sharper decrease compared to the other models for both jumping and skipping activities. The difference between coordination factors between these activities is due to the different motion characteristics in terms of excitation frequency, impact intensity, duration of leg contact with the floor, etc. This leads to distinct behaviour by people in the group in terms of synchronization during movement.

7 Conclusions

An experimental investigation of rhythmic activities on a flexible steel–concrete composite floor is presented in this paper, followed by a numerical analysis to identify the corresponding load models. The investigated rhythmic activities were skipping and jumping and group sizes were between 1 and 32. The major outcomes of this study are summarized as follows:

- A frequency-domain load model characterizing rhythmic activities is proposed. The parameters of this model were determined from experimental acceleration measurements on the tested floor using least-squares identification methods. Each rhythmic activity had a specific set of parameters depending on its style of motion.
- The effect of crowd size (translated by the lack of synchronization between individuals) was investigated by computing RMS forces from the identified spectral load models and deducing corresponding coordination factors. The proposed expressions for these factors comprise a decreasing exponential up to a group size N_0, followed by a constant plateau for larger groups. These relations can be used in combination with the proposed load model of a single person to define the total crowd load model for skipping and jumping activities.
- The accuracy of the proposed coordination factors related to previously identified RMS forces is demonstrated. Moreover, a comparison of these factors with existing results from the literature reveals less conservative results, especially for jumping, whereas more conservative factors are noted for skipping for larger crowds (over 16 persons).

These results constitute a contribution to previous research works paving the way for the development of a simple yet reliable serviceability assessment method of human comfort for multiple usages of floors (sports venues, fitness centres, gymnasiums, grandstands, etc.).

It should be noted that the proposed model is applied for a low density of participants (below 0.3 person/m²) and a group size between 1 and 32. As a future perspective, additional tests involving other rhythmic activities, and performed under more controlled conditions, could be carried out to investigate the group effect considering a wider range of crowd sizes. Correlation of motion between participants might also be analysed for the case of higher densities (more than 0.3 person/m²), and inter-subject variability could be further investigated for different individuals and excitation frequencies.

Acknowledgments

This research was funded by the *Centre Technique Industriel de la Construction Métallique* (CTICM). The authors would like to thank all volunteers who took part in the floor vibration tests.

References

[1] An Q., Ren Q., Liu H., Yan X., Chen Z., Dynamic performance characteristics of an innovative Cable Supported Beam Structure–Concrete Slab Composite Floor System under human-induced loads, Engineering Structures, Vol. 117, p. 40–57, 2016.

[2] Lee K., Lee S.H., Kim G.C., Woo S.S., Global vertical resonance phenomenon between steel building and human rhythmic excitations, Journal of Constructional Steel Research, Vol. 92, p. 164-174, 2014.

[3] Comer A.J., Williams M.S., Blakeborough A., Experimental determination of crowd load and coherency when jumping on a rigid raked grandstand, 25th International Modal Analysis Conference, Orlando, Florida, 19-22 February 2007.

[4] Pernica G., Dynamic load factors for pedestrian movements and rhythmic exercises, Canadian Acoustics, Vol. 18, No. 2, p. 3-3, 1990.

[5] ISO 10137: Bases for design of structures - Serviceability of buildings and walkways against vibration, ISO, 2007.

[6] Ebrahimpour A., Sack R.L., Design live loads for coherent crowd harmonic movements, Journal of Structural Engineering, Vol. 118, No. 4, p. 1121 -1136, 1992.

[7] Parkhouse J.G., Ewins D.J., Crowd-induced rhythmic loading, Proceedings of the Institution of Civil Engineers-Structures and Buildings, Vol. 159, No. 5, p. 247-259, 2006.

[8] da Silva J.G.S., de Andrade S.A.L., da Silva Vellasco P.C.G., de Lima L.R.O., de Almeida R.R., Vibration Analysis of Long Span Joist Floors Submitted to Human Rhythmic Activities, Advances in Vibration Analysis Research, Vol. 231, 2011.

[9] Liu Y., Wang L., Li M., Wu Z., A distributed dynamic load identification method based on the hierarchical-clustering-oriented radial basis function framework using acceleration signals under convex-fuzzy hybrid uncertainties, Mechanical Systems and Signal Processing, Vol. 172, 108935, 2022.

[10] Liu Y., Wang, L., Quantification, localization, and reconstruction of impact force on interval composite structures, International Journal of Mechanical Sciences, Vol. 239, 107873, 2023.

[11] Maes K., Smyth A.W., De Roeck G., Lombaert, G., Joint input-state estimation in structural dynamics, Mechanical Systems and Signal Processing, Vol. 70, p. 445-466, 2016.

[12] Van Nimmen K., Maes K., Van den Broeck P., De Roeck G., Lombaert G., Inverse identification of pedestrian-induced loads, 27th International Conference on Noise and Vibration Engineering, Leuven, Belgium, 19-21 September 2016.

[13] Sedehi O., Papadimitriou C., Teymouri D., Katafygiotis L.S., Sequential Bayesian estimation of state and input in dynamical systems using output-only measurements, Mechanical Systems and Signal Processing, Vol. 131, p. 659-688, 2019.

[14] Teymouri D., Sedehi O., Katafygiotis L.S., Papadimitriou, C., A new online Bayesian approach for the joint estimation of state and input forces using response-only measurements. 13th International Conference on Applications of Statistics and Probability in Civil Engineering, Seoul, South Korea, 26-30 May 2019.

[15] De Silva S., Thambiratnam D., Vibration characteristics of concrete-steel composite floor structures, ACI Structural Journal, Vol. 108, No. 6, p. 706-714, 2011.

[16] Costa-Neves L.F., da Silva J.S., De Lima L.R.O., Jordão S., Multi-storey, multi-bay buildings with composite steel-deck floors under human-induced loads: The human comfort issue, Computers and Structures, Vol. 136, p. 34-46, 2014.

[17] Liu Y., Wang L., A two-step weighting regularization method for stochastic excitation identification under multi-source uncertainties based on response superposition-decomposition principle, Mechanical Systems and Signal Processing, Vol. 182, 109565, 2023.

[18] Xiong J., Chen J., Random field model for crowd jumping loads, Structural safety, Vol. 76, p. 197-209, 2019.

[19] El Asri Y., Lukić M., Hjiaj M., Couchaux M., Denoël V., Crowd size effect on floor vibration response due to random and rhythmic excitations, 27th International Congress on Sound and Vibration ICSV, Online, 12-14 July 2021.

[20] Piersol A., Paez T., Harris' shock and vibration handbook, 6th ed. New York: McGraw-Hill Handbooks, 2001.

[21] Ellis B.R., Ji T., Loads generated by jumping crowds: experimental assessment, BRE IP4/02, CRC Ltd., London, p. 1-12, 2002.

[22] Smith A.L., Hicks S.J., Devine P.J., Design of Floors for Vibration: A New Approach (Revised Edition, February 2009), SCI publication P354, The Steel Construction Institute, 2009.

[23] Ferrarotti A., Tubino, F., Generalized equivalent spectral model for serviceability analysis of footbridges, Journal of Bridge Engineering, Vol. 21, No. 6, 2016.

[24] Racic V., Pavic A., Mathematical model to generate near-periodic human jumping force signals, Mechanical Systems and Signal Processing, Vol. 24, No. 1, p. 138-152, 2010.

[25] Preumont A., Random vibration and spectral analysis, Kluwer Academic, 1994.

[26] Ellis B.R., Littler J.D., Response of cantilever grandstands to crowd loads. Part 2: load estimation, Proceedings of the Institution of Civil Engineers-Structures and Buildings, Vol. 157, No. 5, p. 297-307, 2004.

[27] Gaspar C.M., da Silva J.G.S., Influence of the human rhythmic activities modelling on the composite floors dynamic response, Journal of Civil Engineering and Architecture Research, Vol. 2, No.1, p. 429-437, 2015.